

Relaxed Earth Mover’s Distances for Chain- and Tree-connected Spaces and their use as a Loss Function in Deep Learning

Manuel Martinez*, Monica Haurilet*, Ziad Al-Halah*, Makarand Tapaswi†, Rainer Stiefelhagen*

*Computer Vision for Human-Computer Interaction Lab
Institute for Anthropomatics and Robotics
Karlsruhe Institute of Technology

cvhci.anthropomatik.kit.edu

†Machine Learning Group
Department of Computer Science
University of Toronto

makarand@cs.toronto.edu

Abstract

The Earth Mover’s Distance (EMD) computes the optimal cost of transforming one distribution into another, given a known transport metric between them. In deep learning, the EMD loss allows us to embed information during training about the output space structure like hierarchical or semantic relations. This helps in achieving better output smoothness and generalization. However EMD is computationally expensive. Moreover, solving EMD optimization problems usually require complex techniques like lasso. These properties limit the applicability of EMD-based approaches in large scale machine learning.

We address in this work the difficulties facing incorporation of EMD-based loss in deep learning frameworks. Additionally, we provide insight and novel solutions on how to integrate such loss function in training deep neural networks. Specifically, we make three main contributions: (i) we provide an in-depth analysis of the fastest state-of-the-art EMD algorithm (Sinkhorn Distance) and discuss its limitations in deep learning scenarios. (ii) we derive fast and numerically stable closed-form solutions for the EMD gradient in output spaces with chain- and tree- connectivity; and (iii) we propose a relaxed form of the EMD gradient with equivalent computational complexity but faster convergence rate. We support our claims with experiments on real datasets. In a restricted data setting on the ImageNet dataset, we train a model to classify 1000 categories using 50K images, and demonstrate that our relaxed EMD loss achieves better Top-1 accuracy than the cross entropy loss. Overall, we show that our relaxed EMD loss criterion is a powerful asset for deep learning in the small data regime.

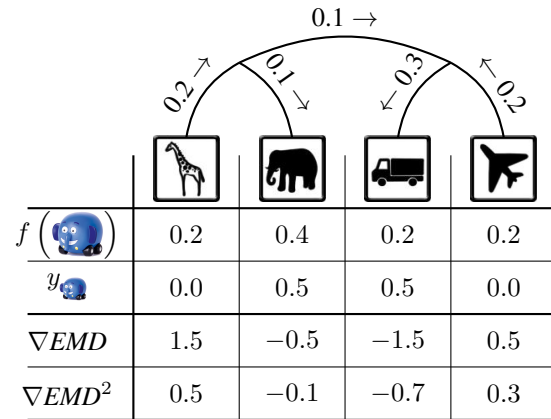


Figure 1: We train a deep learning model using *Ellyvan* (a hybrid elephant and van). The output of the forward pass is presented in the first row, and the label in the second. The tree-structured output space allows us to train the network using gradients from the Earth Mover’s Distance (∇EMD). We introduce a regularized form that converges faster (∇EMD^2) and is more stable.

1. Introduction

The Wasserstein metric [33] is a distance function based on the optimal transport problem that compares two data distributions. While computing such metrics on digital devices, it is common practice for data distributions to work in a discretized space (e.g. arranged in bins). Here, the Wasserstein distance is popularly known as the Earth Mover’s Distance (EMD) [24]. The name is derived from a visual analogy of the data distributions as two piles of dirt (earth). EMD is defined as the minimum amount of effort required to make both distributions look alike. Note that the individual bins of both distributions should be non-negative and their total mass equal (as is the case with probability distributions).

The EMD is widely used to compare histograms and

probability distributions [16, 20, 23, 24, 25]. However, calculating the *EMD* is known to be computationally expensive. This has led to several relaxed versions of the *EMD* for cases where speed is critical, *e.g.* when comparing feature vectors [14, 19, 21].

In addition to the large computational cost, *EMD* has the drawback of an ℓ_1 behavior. Solving *EMD* optimization problems often require *lasso* optimization techniques (*e.g.*, mirror descent, Bregman projections, etc.). This represents a significant drawback for current deep learning approaches that strongly favor gradient-based methods such as Stochastic Gradient Descent, Momentum [31], and Adam [2], that provide several small updates to the model parameters.

Sinkhorn Distance. Using the *EMD* within an iterative optimization scheme was made feasible by Cuturi [7], who realized that an entropically regularized *EMD* can be efficiently calculated using the Sinkhorn-Knopp [27] algorithm. The resulting is referred to as the Sinkhorn Distance (*SD*), and has achieved wide popularity within a number of learning frameworks [3, 4, 9, 10, 18, 22, 23, 28, 29, 30]. The *SD* approximates *EMD* effectively, and provides a subgradient for the *EMD* as a side result of the estimation. This *SD* subgradient has been used to train deep learning models [10] and is implemented as a loss criterion in popular deep frameworks such as Caffe [12] and Mocha [1]. However, as *SD* is an ℓ_1 norm, Frognier *et al.* [10] need to combine *SD* with the Kullback-Leibler divergence and use an exceedingly small learning rate for it to converge.

Furthermore, the *SD* algorithm is prone to numerical instabilities when used in deep learning frameworks. In some conditions, these instabilities imply that *SD* is not a close approximation of *EMD*. We believe that an analysis of the causes of instabilities is critical to extend the use of *SD* to deep learning frameworks and discuss them in detail in Sec. 2.

Earth Mover’s Distance. Concurrently, we suggest an alternative approach to *SD*. Instead of tackling the general case, we focus on output spaces whose connectivity graph takes the form of a chain (histograms or probability distributions) or a tree (hierarchies). We provide closed-form solutions for the real *EMD* and its gradient.

We start with chain-connected distributions (see Fig. 4) that have a well-known closed-form solution [32], and derive its gradient. We also propose a relaxed version of the *EMD*, named *EMD*² that exhibits similar structure but converges faster due to its ℓ_2 behavior.

Furthermore, we derive a closed form solution for the *EMD* and its gradient that is valid for all metric spaces that have a tree connectivity graph. This allows us to represent complex output spaces that are hierarchical in nature (*e.g.*, WordNet [17] and ImageNet [26], Sentence Parse Trees [15]). We see an example of a hierarchical output space of object categories in Fig. 1. We depict the expected

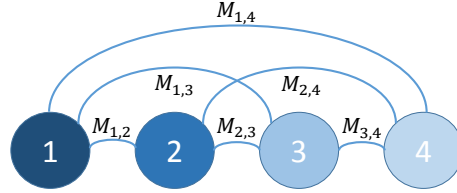


Figure 2: We illustrate the general case of the *EMD*, where the *dirt* can be moved from and to all bins directly. Computing the amount of *dirt* that goes (flows) through each path is computationally expensive.

flow of *dirt* on the tree branches, and present the gradients for both original and relaxed versions of the *EMD* (details of the gradients in Sec. 3.2 and Sec. 4).

EMD as a loss criterion for deep learning. Using *EMD* as a loss criterion has several unique advantages over unstructured losses. It allows us to shape the output relationships we expect from a model. For example, it can tell the model that confusing a cat for a tiger may more acceptable than confusing a cat for a starship, and thus adds knowledge to the model. Additionally, *EMD* gradients (in contrast to *MSE*) are holistic and affect the whole output space as it is connected. Therefore, models that predict the entire output space (*e.g.*, histograms) converge faster.

Overall, we see that *EMD* has the effect of magnifying the information that an input data sample provides. Each input sample does not only provide information about its own class, but also contains the relationship it has with the rest of the output bins (*e.g.*, classes, histogram bins, etc.) This second source of information helps generalize better, and results in improved performance with less data.

We demonstrate these characteristics in two real-world experiments. We train a model to predict the Power Spectral Density of respiratory signals of sleep laboratory patients. In this setting the *EMD* converges faster than the *SD* and *MSE* losses, and achieves better accuracy. Our second experiment is performed on a reduced version of the ILSVRC 2012 challenge [26]. We use all 1000 categories, but limit the training data to 50K images. This, along with the *EMD* criterion, forces the network to learn the output space hierarchy. While *EMD* alone is not enough to achieve the best top-1 accuracy, an equal combination of *EMD* and cross entropy loss achieves better top-1 accuracy than using cross entropy alone.

2. The Earth Mover’s Distance

As discussed earlier, the *EMD* is defined for discrete distributions. Here, the probability mass (or *dirt*) is distributed in discrete piles or bins. The effort of moving a mound of *dirt* between two bins is a non-negative cost which is linearly proportional to the amount of *dirt* and distance between the

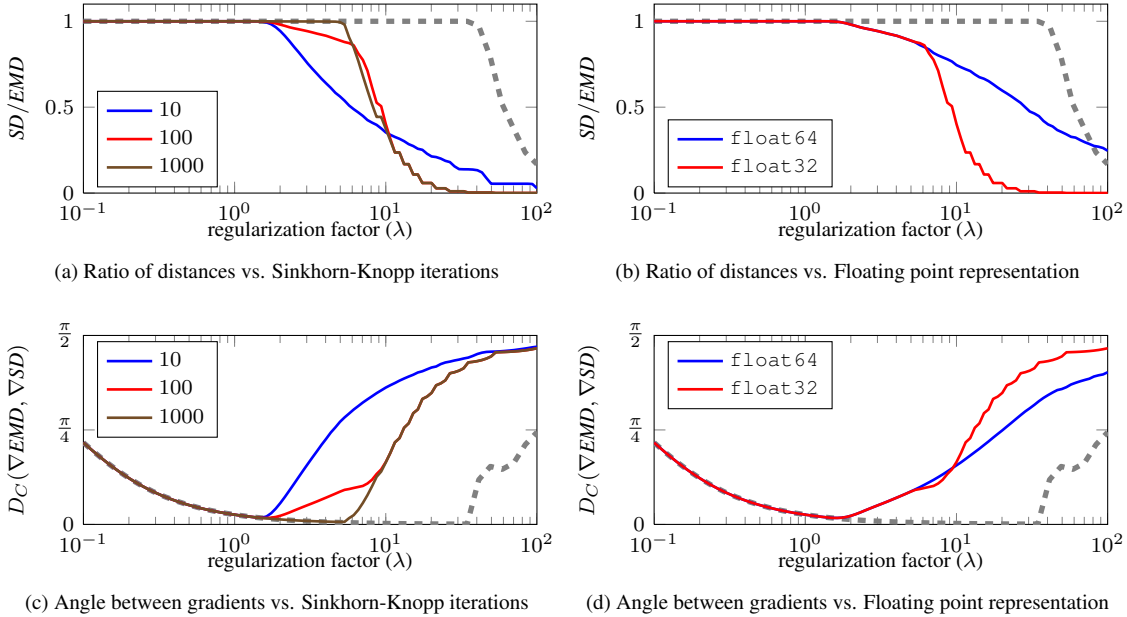


Figure 3: We show how implementation and hyper-parameter choices affect SD with an experiment on the WordNet hierarchy for 1000 ImageNet classes. (a,b): Ratio of SD to the real EMD . (c,d): Angle of the cosine distance ($D_C(\cdot, \cdot)$) between EMD and SD gradients. (a,c): Impact of limiting Sinkhorn-Knopp iterations. We see that larger values of λ require a large amount of iterations to converge (two typical values used in deep learning are 10 [10] and 100 [12]). (b,d): `float32` (GPU) has a reduced dynamic range compared to `float64` (CPU), which degenerates for large λ values. The gray dashed line shown as a reference, corresponds to 10000 iterations using `float64` representation. The most commonly cited value of λ is 10.

bins.

Within this discrete domain, the general form of EMD between two distributions $\mathbf{p}, \mathbf{q} \in \mathbb{R}_+^N$ with $\|\mathbf{p}\|_1 = \|\mathbf{q}\|_1$ is

$$EMD(\mathbf{p}, \mathbf{q}) = \inf_{T \in U(\mathbf{p}, \mathbf{q})} \langle M, T \rangle, \quad (1)$$

where $\langle \cdot, \cdot \rangle$ is the Frobenius inner product and $M \in \mathbb{R}_+^{N \times N}$ defines the generalized distance between bins (see Fig. 2). $U(\mathbf{p}, \mathbf{q})$ is the set of valid transport plans between \mathbf{p} and \mathbf{q} ,

$$U(\mathbf{p}, \mathbf{q}) = \{T \in \mathbb{R}_+^{N \times N} : T \cdot \mathbf{1}_N = \mathbf{p}, T^\top \cdot \mathbf{1}_N = \mathbf{q}\}. \quad (2)$$

$\mathbf{1}_N$ is an N dimensional vector of all ones, and T is constrained such that its row sum corresponds to the distribution \mathbf{p} and column sum to \mathbf{q} .

Without loss of generality (a simple scalar normalization), in the rest of the paper we assume $\|\mathbf{p}\|_1 = \|\mathbf{q}\|_1 = 1$.

2.1. Unnormalized distributions

The original EMD is not defined for $\|\mathbf{p}\|_1 \neq \|\mathbf{q}\|_1$. Although there are several ways to modify the EMD for unnormalized distributions [5, 10, 19] we consider that this goes against the spirit of the metric. Therefore, prior to computing the EMD , we ℓ_1 -normalize the input distributions either using a ℓ_1 normalization layer, or a *softmax* layer.

2.2. Sinkhorn distance

The general formulation of the EMD (Eq. 1) is solved using linear programming which is computationally expensive. However, this problem was greatly alleviated by Cuturi [7] who suggested a smoothing term for the EMD in the form of

$$SD_\lambda(\mathbf{p}, \mathbf{q}) = \inf_{T \in U(\mathbf{p}, \mathbf{q})} \langle M, T \rangle - \frac{1}{\lambda} \langle T, \log T \rangle, \quad (3)$$

which allows to use the Sinkhorn-Knopp algorithm [27] to obtain an iterative and efficient solution.

The Sinkhorn-Knopp algorithm is notable as it converges fast and produces a subgradient for the SD without extra cost. This subgradient can in turn be used to update parameters of machine learning models [10]. The algorithm is defined as¹:

2.3. Numerical stability of the Sinkhorn Distance

We claim that the SD is not numerically stable when used in common deep learning frameworks. We substantiate this claim by comparing the output of the SD and its gradient to the real EMD . We extract a hierarchy of categories from the WordNet ontology for the 1000 classes of the ILSVRC2012

¹Of the several variants of the algorithm, this follows the one in Caffe [12]. \odot and \oslash stand for per-element multiplication and division respectively.

Algorithm 1 Sinkhorn Distance and Gradient

Require: $f(x), y, \lambda, \mathbf{M}$
 $\mathbf{K} \leftarrow e^{-\lambda \mathbf{M}^{-1}}, u \leftarrow \mathbf{1}, it \leftarrow 1$
while not converged **and** it \leq MAX-ITER **do**
 $u \leftarrow f(x) \odot (\mathbf{K}(y \odot \mathbf{K}^\top u))$
end while
 $v \leftarrow y \odot (\mathbf{K}^\top u)$
 $SD \leftarrow \text{sum}(u \odot (\mathbf{K} \odot \mathbf{M}v))$
 $\nabla SD \leftarrow \log u / \lambda$

dataset [26]. The tree has 1374 nodes in total. This hierarchy acts as the structure of the output space in our evaluation.

There are three parameters that impact numerical stability of the SD in deep learning:

Iteration limit: any practical implementation needs an upper limit for the number of SD iterations. This leads to a trade-off between speed and accuracy which is more apparent for larger values of λ , as seen in Fig. 3 (a), (c).

Floating point accuracy: the Sinkhorn algorithm alternately normalizes rows and columns of the transport matrix. This requires several multiply-accumulate operations which are prone to numerical inaccuracies. This problem is made worse by the exponential form of $\mathbf{K} = e^{-\lambda \mathbf{M}^{-1}}$, which increases the dynamic range of the values. To make things worse, GPUs use a `float32` representation, instead of the common `float64` representation used by CPUs. In Fig. 3 (b) and (d), we observe how using `float32` affects the results, especially for large values of λ where more iterations are required to converge.

Regularization factor (λ): the regularization factor affects both the accuracy and the convergence behavior of SD . In a non-deep learning framework, the number of iterations does not pose a limit and `float64` representation can be used. Lower values of λ imply better convergence behavior [8], while larger values approximate the Earth Mover’s Distance better (see gray reference line in Fig. 3). However, in deep learning applications where `float32` representation are common and the iteration number is typically chosen to be 10 [10] or 100 [12], larger values of λ are unusable.

In general, SD works best when the ratio between the largest and the smallest non-zero value in the \mathbf{M} is small (thus has a smaller dynamic range), and the size of the output space is small (due to the reduced number of multiply-add operations).

3. EMD in chain-connected spaces

We analyze the scenario where bins in a distributions (e.g. histograms, probabilities) are situated in a one dimensional space. Here, moving *dirt* from a source to target bin

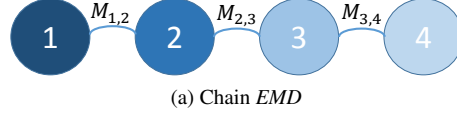


Figure 4: One dimensional probability distributions are a perfect example of chain output spaces. In chains, *dirt* must travel through all intermediate bins in its path. This greatly simplifies the computation of the EMD , as it only requires to eliminate one node and edge at each step.

requires an ordered visit to every bin in between (see Fig. 4).

The bin distance M can be defined recursively to ensure that only consecutive bin distances are considered.

$$M_{i,j} = \begin{cases} 0 & \text{if } i = j, \\ M_{i-1,j} + d_{i-1,i} & \text{if } i > j, \\ M_{j,i} & \text{if } i < j. \end{cases} \quad (4)$$

Here, $d_{i-1,i}$ is the distance between two consecutive bins (typically all equal and 1).

The above choice of bin distances facilitates a simple solution to calculate the EMD using a recursion. Essentially, each bin either receives all the excess *dirt* that results from leveling previous bins, or in case of a deficit, tries to provide for it. Note that the cost of going left-to-right ($M_{i,j}$) or right-to-left ($M_{j,i}$) is symmetric. The closed form recursive formulation for the EMD between two one-dimensional distributions is:

$$\overrightarrow{EMD}(\mathbf{p}, \mathbf{q}) = \sum_{i=1}^{N-1} M_{i,i+1} \cdot |\varphi_i|, \quad (5)$$

where φ_i represents the excess *dirt* that needs to be moved ahead or deficit in *dirt* that needs to be filled up to bin i .

$$\varphi_i = \sum_{j=1}^i (p_j - q_j). \quad (6)$$

For notational brevity, we will refer to $M_{i,i+1}$ as \hat{M}_i . The above expression can be rewritten with the sign function as

$$\overrightarrow{EMD}(\mathbf{p}, \mathbf{q}) = \sum_{i=1}^{N-1} \hat{M}_i \cdot \text{sgn}(\varphi_i) \cdot \varphi_i. \quad (7)$$

Note that as both distributions have the same amount of total mass, and we progressively level out the *dirt* over all bins, when we arrive to the last bin all *dirt* will have been leveled (i.e. $\varphi_N = 0$). Therefore, we compute the outer sum only up to $N - 1$.

3.1. Gradient of the Earth Mover’s Distance

To integrate EMD as a loss function in an iterative gradient-based optimization approach, we need to compute

the analytical form of the gradient. However, we must ensure that the gradient obeys the law of *dirt* conservation. The gradient should not create new or destroy existing *dirt* to avoid changing the total mass of the distributions ($\|\mathbf{p}\|_1 \neq 1$ after updates).

We use the trick of projected gradients, and define \mathbf{e}_k as a vector of length N whose value at entry k is $1 - 1/N$, and $-1/N$ elsewhere. Note that \mathbf{e}_k sums to 0. For a small value h , we compute the distance between the perturbed distribution $\mathbf{p} + h\mathbf{e}_k$ and \mathbf{q} as:

$$\overrightarrow{EMD}(\mathbf{p} + h\mathbf{e}_k, \mathbf{q}) \simeq \sum_{i=1}^{N-1} \hat{M}_i \cdot \text{sgn}(\varphi_i) \sum_{j=1}^i (p_j + h(\delta_{jk} - 1/N) - q_j), \quad (8)$$

where $\delta_{jk} = 1$ iff $j = k$. Note that by choosing h small enough, $\text{sgn}(\varphi_i)$ can be assumed to remain unchanged. The corresponding partial derivative for the \overrightarrow{EMD} is:

$$\frac{\partial \overrightarrow{EMD}(\mathbf{p}, \mathbf{q})}{\partial p_k} \simeq \sum_{i=1}^{N-1} \hat{M}_i \cdot \text{sgn}(\varphi_i) \sum_{j=1}^i (\delta_{jk} - 1/N). \quad (9)$$

3.2. Relaxed Earth Mover's Distance

The proposed gradient (Eq. 9) is numerically stable and avoids erosion or addition of new dirt. This is an important step forward to use *EMD* in learning frameworks.

However, as the distance contains an absolute value function ($|\varphi_i|$) we observe difficulties converging to a solution, similar to ℓ_1 optimization. In particular, when $\hat{M}_i \in \mathbb{N}$, it is easy to see that the terms of ∇EMD are integer fractions of N (see Fig. 1, multiples of 0.25). Furthermore, as small changes to the distribution do not change the gradient, the Hessian is zero except at a few discrete set of points (where the sign of φ_i changes) making optimization hard.

To solve these issues, we suggest a relaxed form of the *EMD* where the cost is calculated proportional to a power of the excess/deficit of *dirt*.

$$\overrightarrow{EMD}^\rho(\mathbf{p}, \mathbf{q}) = \sum_{i=1}^{N-1} \hat{M}_i \cdot |\varphi_i|^\rho. \quad (10)$$

whose gradient is:

$$\nabla \overrightarrow{EMD}^\rho \simeq \rho \sum_{i=1}^{N-1} \hat{M}_i \cdot \varphi_i \cdot |\varphi_i|^{\rho-2} \sum_{j=1}^i (\delta_{jk} - 1/N). \quad (11)$$

For $\rho = 1$ we have the normal *EMD* distance, which behaves like ℓ_1 . During gradient descend we suggest to use the case with $\rho = 2$ that bears similarity with the popular Mean Squared Error loss. EMD^2 preserves the nice properties of conserving dirt, while having real valued gradients

(see an example in Fig. 1). In addition, we see that \overrightarrow{EMD}^2 also exhibits non-zero Hessians.

$$\frac{\partial^2 \overrightarrow{EMD}^2(\mathbf{p}, \mathbf{q})}{\partial p_k \partial p_l} = 2 \sum_{i=1}^{N-1} \hat{M}_i \cdot (N \cdot H(i-l) - i) \cdot (N \cdot H(i-k) - i), \quad (12)$$

where $H : \mathbb{R} \rightarrow \{0, 1\}$ is the Heaviside step function defined as $H(n) = \{1 \text{ if } n \geq 0, 0 \text{ otherwise}\}$.

3.3. Discussion: comparing *EMD*, *SD* and *MSE*

Plotting the gradients provides a good impression of the actual behavior of the *EMD*. It also shows how *EMD* serves as a criterion that provides holistic optimization over the output space (full distribution).

In Fig. 5 we show the gradients corresponding to several different loss criteria for the transformation between two unit-norm distributions: a smooth one \mathbf{p} , and a spiky one \mathbf{q} . We present the gradient of *MSE* in Fig. 5 (a). Note how *MSE* optimizes each bin independently, and results in a non-smooth gradient.

In Fig. 5 (b) we show the gradients for *EMD* and EMD^2 . In both cases the gradient is holistic and affects the whole output space. Furthermore, the regularization effect induced by EMD^2 results in a smoother gradient.

In Fig. 5 (c) we show the *SD* gradient for λ values of 0.5, 1 and 10. In all cases the gradients are also holistic. We see that larger values of λ produce a gradient resembling that of the true *EMD*, however it comes with its own set of problems that were discussed earlier.

4. *EMD* in tree-connected spaces

We demonstrate here how *EMD* can be used to model output spaces with a tree structure. Our formulation expects that all observed bins correspond to the leaves of the tree, and the remaining latent nodes and have no *dirt*. As we can link a tree to any non-leaf node with a zero-cost connection, this formulation allows us to express any tree structure. We refer to this analysis as the Hierarchical Earth Mover's Distance (*HEMD*) (see Fig. 1). Note that, this is still compatible with all our previous developments (as chains are a sub-class of trees). As such, we do not distinguish between *EMD* and *HEMD* while presenting the evaluation.

We define $HEMD^\rho$ as:

$$HEMD^\rho(\mathbf{p}, \mathbf{q}) = \sum_{i \in G} M_{i, \mathbf{p}(i)} \cdot |\tilde{\varphi}_i|^\rho, \quad \text{where} \quad (13)$$

$$\tilde{\varphi}_i = \sum_{j \in \mathbf{l}(i)} (p_j - q_j), \quad (14)$$

where $M_{i, \mathbf{p}(i)}$ is the cost of transporting *dirt* from node i to its parent (abbreviated as \tilde{M}_i), G is the set of all nodes in the

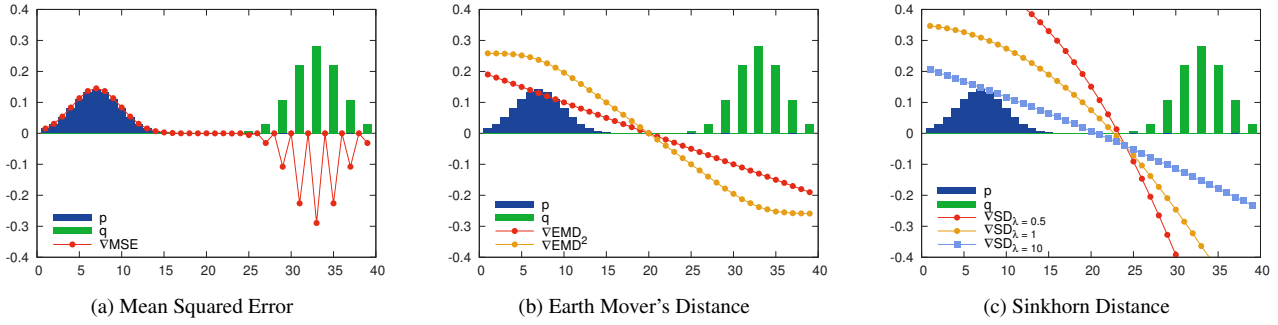


Figure 5: Gradient flow to convert a source distribution \mathbf{p} to a target \mathbf{q} . (a) MSE gradient is not smooth, and does not affect the whole output space. (b) EMD and EMD^2 gradients affect the whole space. EMD^2 has ℓ_2 behavior, while EMD behaves like ℓ_1 . (c) SD gradients also affect the whole space but the regularized versions are asymmetric. $SD_{\lambda=10}$ approximates EMD well.

tree, and $\mathbf{I}(i)$ is the set of all leaves in the subtree that has i as a root. N is the total number of leaves (and bins) in the tree. The intuition behind this formula is that we can reduce the tree one leaf at a time as if it were the tail of a chain.

Then the gradient of $HEMD$ is defined as:

$$\nabla HEMD^\rho \simeq \rho \sum_{i \in G} \tilde{M}_i \cdot \tilde{\varphi}_i \cdot |\tilde{\varphi}_i|^{\rho-2} \sum_{j=1}^i (\delta_{jk} - 1/N). \quad (15)$$

All equations can be solved efficiently by a post-order traversal of nodes in the tree.

5. Experimental analysis

We implement our models, the EMD and the SD criteria using Torch [6]². Evaluation is performed on an i5-6600K CPU at 3.5GHz with 64GB of DDR4-2133 RAM and a GTX1080 GPU running Ubuntu 16.04, CUDA 8.0 and cuDNN 5.1.3. Unless otherwise stated, the SD hyperparameters are $\lambda = 3$, the iteration limit 100, and using CUDA (*i.e.* float32 type).

5.1. Timing analysis for SD vs. EMD^2

We evaluate the computational efficiency of EMD^2 and SD . The Sinkhorn-Knopp algorithm is very efficient and demonstrates fast GPU performance. However, being an iterative procedure, SD is significantly slower than EMD^2 (see Table. 1). Furthermore, it is not practical for large output spaces, especially if we require the use of float64 precision which is only available on CPUs.

5.2. EMD^2 on Chain Spaces

We evaluate the use of EMD to learn Power Spectral Density (PSD) - a chain distribution with signal power binned

	max iter.	CPU	GPU
SD	10	942ms	15.1ms
SD	100	7.51s	88.9ms
SD	1000	74.5s	865ms
EMD^2	-	126ms	25ms

Table 1: Computation time for the gradients of SD and EMD^2 on the WordNet Tree Structure experiment for one minibatch of size 512. The closed form solution allows the EMD^2 to be 60x faster to calculate than 100 iterations of SD on a CPU. Our unoptimized CUDA code is 3.5x faster than SD . Note that it is not practical to run SD on float64 precision and 1000 iterations, as it takes 74 seconds to evaluate the loss for a single minibatch.

into different frequencies. As we need to optimize over the whole output space, this task is not only well-suited to use EMD as a loss criterion, but EMD also serves as the evaluation metric.

Our task is to predict the PSD of a breathing signal obtained from a patient using chest excursion signals (a nose thermistor acts as reference). Our data is recorded from 75 real patients from a sleep laboratory. We extract 200 one-minute clips for each patient, providing us with a dataset of 15,000 samples. We use data from 60 patients to train our models, and the remaining 15 as test subjects.

Noise levels depend on the activity of the patient, and are negligible when he/she is relaxed. On the other hand, when the patient moves, sits, or talks during the 1 minute segment, the correlation between chest movement and respiration disappears.

We adopt a two layer network for this experiment. The first layer consists of 16 temporal convolution filters with a receptive field of 11. We apply the \tanh nonlinearity, and stack a fully connected layer on top. To ensure positive outputs (as we predict signal power) we apply the *square*

²Code will be made publicly available

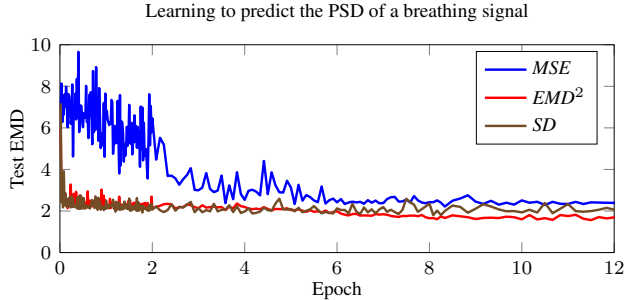


Figure 6: We train a regressor to estimate the PSD of real breathing signals obtained from chest excursions. We observe that both EMD^2 and SD learn the transformation significantly faster than the MSE . Over a longer period EMD^2 achieves better accuracy than SD .

function $(\cdot)^2$ to the output layer. We use the *Adam* optimizer [2].

On this simple task *Adam* performs very well, and the model converges with all criteria (see Fig. 6). Nevertheless, both EMD^2 and SD outperform MSE , converging in a fraction of the first epoch.

This highlights the benefits of using EMD criterion in cases where it can be hard to obtain several training samples and the output space has a suitable structure.

5.3. EMD^2 on Tree Spaces

To evaluate the EMD^2 loss on a hierarchical space, we develop an experiment based on the well known 1000-class ImageNet object recognition challenge [26].

We train a model similar to Alexnet [13] with batch normalization [11] after ReLU, using a minibatch size of 512, a learning rate of 0.05 with a decay of 10^{-5} and a ℓ_2 weight penalty of 10^{-4} . We use Stochastic Gradient Descent (SGD) as optimizer with momentum of 0.9. The input image is downsized to 112×112 pixels, and horizontal flipping and cropping is used for data augmentation at train time only.

The output space hierarchy tree is obtained from WordNet [17] and has a total of 1374 nodes and a maximum distance between nodes of 26. We set all edge costs to 1. By our definition, the output labels correspond to the leaves of the tree. Thus, the minimum hierarchical distance between a pair of output labels is 2.

We evaluate the following loss criteria:

Cross Entropy (CE): the standard loss used in classification problems and state-of-the-art ImageNet models.

EMD^2 : pure EMD^2 after a softmax non-linearity.

$EMD^2 + CE$: a 1 : 1 combination of EMD^2 and CE .

$SD + CE$: a 1 : 3 combination of SD and CE . We give more emphasis to CE since using a 1 : 1 ratio did not converge.

SD and EMD alone do not converge using SGD on a large

variation of parameter combinations that we tried. This is somewhat expected behavior for ℓ_1 losses.

We explore two data setups. In the first case, the full training set is available (1280K images), while in the second, only a small amount of training data is available ($\sim 4\%$, 50K images). Our results show little advantage for EMD when using the full training set (see Fig. 7 (a)). This happens because the model can already learn the output space hierarchy from the input images used for training. However, obtaining such large datasets is a daunting task.

We discuss the results at more depth for the second setting with reduced data (50K images). As metrics, we present the Top-1 accuracy and the EMD loss. Top-1 accuracy is a common metric used in the ImageNet challenge which depends only on the largest value of the output vector. On the other hand, the EMD loss has an opposite notion, as it depends on the output of the entire vector.

CE loss: The CE loss strongly favors Top-1 accuracy, and thus converges the fastest with regards to the Top-1 metric (see Fig. 7 (a) and (b)). When operating in the reduced data setting, improvements in Top-1 accuracy have the side effect of reducing the holistic loss (Fig. 7 (c)) as the model also begins to learn the leaves of the hierarchical space from the input data. However, the model soon starts over-fitting, the Top-1 accuracy plateaus, and the holistic loss grows back to its original value.

EMD^2 loss: We see an effect opposite to that of CE when using EMD^2 . The EMD^2 loss optimizes primarily for the holistic loss (see Fig. 7 (c)). Here, the improvements in Top-1 accuracy are a side effect and also slow. Nevertheless, we see in Fig. 7 (b) that the Top-1 accuracy of EMD^2 ends up higher than CE in the 50K image setting, as it learns the entire output space.

$EMD^2 + CE$ losses: The combination of losses provides fast network convergence and highest Top-1 accuracy (see Fig. 7 (b)). The CE loss optimizes Top-1 accuracy while the EMD^2 incorporates the information of the output space through the holistic optimization.

$SD + CE$ losses: We see to a lesser extent a similar behavior to that of $EMD^2 + CE$. However, the performance is limited by the fact that SD is mainly an ℓ_1 distance, and the Sinkhorn-Knopp algorithm is not numerically stable for large output spaces with the `float32` representation.

6. Conclusion

SD has achieved wide-spread popularity in applications that wish to optimize for the EMD criterion. However, with a thorough analysis, we point out two limitations in SD which make it hard to use in deep learning: (i) numerical instability due to floating point precision; and (ii) the ℓ_1 behavior that makes it hard to optimize.

We counter this by deriving closed-form solutions for EMD and its *dirt* conserving gradient on chain (e.g. his-

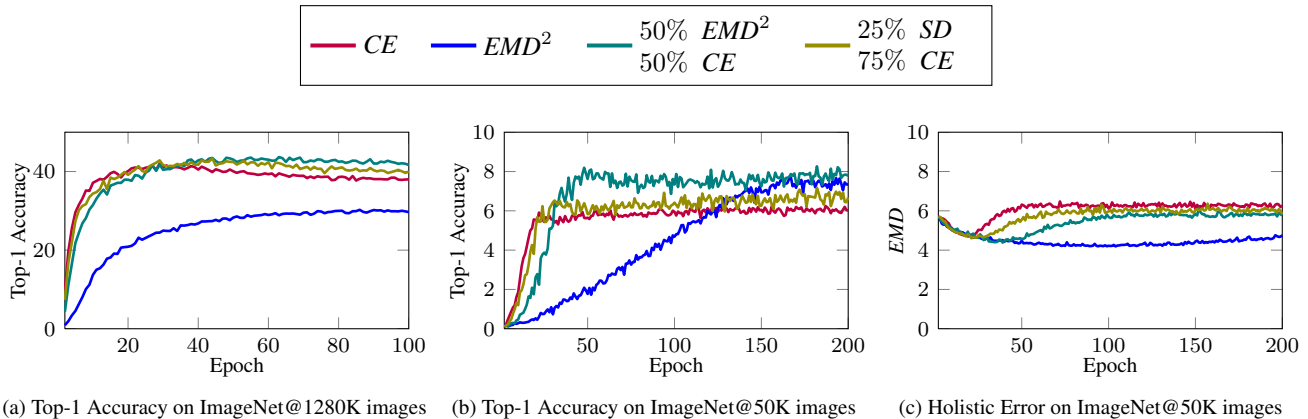


Figure 7: We analyze the use of Earth Mover’s Distance as a loss criterion on the 1000-class ImageNet Large-Scale Visual Recognition Challenge. (a) We evaluate on the full training set, where a combined loss of EMD^2 and Cross Entropy provides the best top-1 accuracy. EMD^2 alone does not achieve high top-1 accuracy as it tries to optimize for the whole output space and not only the best result. (b) We evaluate on 50K images, which is about 4% of the original training set. In this case the improvement provided by EMD^2 criterion is more apparent. (c) We plot the holistic error of the entire output space for the 50K images subset. The EMD^2 outperforms others and its combinations by a large gap.

tograms) and tree (e.g. hierarchies) output spaces. We also propose a relaxed version (EMD^2) of the original distance and compute its analytical form. Our EMD^2 exhibits better properties regarding numerical stability and convergence.

On a task about predicting the PSD of respiratory signals (chain-connectivity), we demonstrate faster convergence and reduction in error using EMD^2 . We also evaluate object categorization on 1000 classes from the ImageNet challenge and work in the regime of limited training data (50K image samples). Here, using the WordNet hierarchy (tree-connectivity), we observe that modeling the output space through the use of EMD^2 helps boost the performance.

Our contributions will help promote a wider adaption EMD as a loss criterion within deep learning frameworks.

References

- [1] Mocha - a Deep Learning Framework for Julia. <https://github.com/pluskid/Mocha.jl>, 2016.
- [2] J. Ba and D. Kingma. Adam: A method for stochastic optimization. In *International Conference on Learning Representations (ICLR)*, 2015.
- [3] J.-D. Benamou, G. Carlier, M. Cuturi, L. Nenna, and G. Peyré. Iterative bregman projections for regularized transportation problems. *SIAM Journal on Scientific Computing*, 37(2):A1111–A1138, 2015.
- [4] N. Bonneel, J. Rabin, G. Peyré, and H. Pfister. Sliced and radon wasserstein barycenters of measures. *Journal of Mathematical Imaging and Vision*, 51(1):22–45, 2015.
- [5] L. Chizat, G. Peyré, B. Schmitzer, and F.-X. Vialard. Unbalanced optimal transport: geometry and Kantorovich formulation. *arXiv preprint arXiv:1508.05216*, 2015.
- [6] R. Collobert, K. Kavukcuoglu, and C. Farabet. Torch7: A matlab-like environment for machine learning. In *BigLearn, NIPS Workshop*, 2011.
- [7] M. Cuturi. Sinkhorn distances: Lightspeed computation of optimal transport. In *Advances in Neural Information Processing Systems (NIPS)*, 2013.
- [8] M. Cuturi and A. Doucet. Fast computation of wasserstein barycenters. In *International Conference on Machine Learning (ICML)*, 2014.
- [9] M. Cuturi and G. Peyré. A smoothed dual approach for variational Wasserstein problems. *SIAM Journal on Imaging Sciences*, 9(1):320–343, 2016.
- [10] C. Frogner, C. Zhang, H. Mobahi, M. Araya, and T. A. Poggio. Learning with a Wasserstein Loss. In *Advances in Neural Information Processing Systems (NIPS)*, 2015.
- [11] S. Ioffe and C. Szegedy. Batch normalization: Accelerating deep network training by reducing internal covariate shift. *arXiv preprint arXiv:1502.03167*, 2015.
- [12] Y. Jia, E. Shelhamer, J. Donahue, S. Karayev, J. Long, R. Girshick, S. Guadarrama, and T. Darrell. Caffe: Convolutional architecture for fast feature embedding. In *ACM Multimedia (MM)*, 2014.
- [13] A. Krizhevsky, I. Sutskever, and G. E. Hinton. ImageNet Classification with Deep Convolutional Neural Networks. In *Advances in Neural Information Processing Systems (NIPS)*, 2012.
- [14] H. Ling and K. Okada. An efficient earth mover’s distance algorithm for robust histogram comparison. *IEEE Transactions on Pattern Analysis and Machine Intelligence (PAMI)*, 29(5):840–853, 2007.
- [15] M. P. Marcus, M. A. Marcinkiewicz, and B. Santorini. Building a Large Annotated Corpus of English: The Penn Treebank. *Computational Linguistics*, 19(2):313–330, 1993.
- [16] S. Marinai, B. Miotti, and G. Soda. Using earth mover’s distance in the bag-of-visual-words model for mathematical

- symbol retrieval. In *International Conference on Document Analysis and Recognition (ICDAR)*, 2011.
- [17] G. A. Miller. WordNet: A Lexical Database for English. *Communications of the ACM*, 38(11):39–41, 1995.
- [18] G. Montavon, K.-R. Müller, and M. Cuturi. Wasserstein Training of Boltzmann Machines. *arXiv preprint arXiv:1507.01972*, 2015.
- [19] O. Pele and M. Werman. Fast and robust earth mover’s distances. In *International Conference on Computer Vision (ICCV)*, 2009.
- [20] S. Peleg, M. Werman, and H. Rom. A unified approach to the change of resolution: Space and gray-level. *IEEE Transactions on Pattern Analysis and Machine Intelligence (PAMI)*, 11(7):739–742, 1989.
- [21] J. Rabin, J. Delon, and Y. Gou. Circular Earth Mover’s Distance for the comparison of local features. In *International Conference on Pattern Recognition (ICPR)*, 2008.
- [22] J. Rabin and N. Papadakis. Convex color image segmentation with optimal transport distances. In *Scale Space and Variational Methods in Computer Vision*, pages 256–269. Springer, 2015.
- [23] A. Rolet, M. Cuturi, and G. Peyré. Fast Dictionary Learning with a Smoothed Wasserstein Loss. In *International Conference on Artificial Intelligence and Statistics (AISTATS)*, 2016.
- [24] Y. Rubner, C. Tomasi, and L. J. Guibas. A metric for distributions with applications to image databases. In *International Conference on Computer Vision (ICCV)*, 1998.
- [25] Y. Rubner, C. Tomasi, and L. J. Guibas. The earth mover’s distance as a metric for image retrieval. *International Journal of Computer Vision (IJCV)*, 40(2):99–121, 2000.
- [26] O. Russakovsky, J. Deng, H. Su, J. Krause, S. Satheesh, S. Ma, Z. Huang, A. Karpathy, A. Khosla, M. Bernstein, A. C. Berg, and L. Fei-Fei. ImageNet Large Scale Visual Recognition Challenge. *International Journal of Computer Vision (IJCV)*, 115(3):211–252, 2015.
- [27] R. Sinkhorn. Diagonal equivalence to matrices with prescribed row and column sums. *The American Mathematical Monthly*, 74(4):402–405, 1967.
- [28] J. Solomon, F. De Goes, G. Peyré, M. Cuturi, A. Butscher, A. Nguyen, T. Du, and L. Guibas. Convolutional wasserstein distances: Efficient optimal transportation on geometric domains. *ACM Transactions on Graphics (TOG)*, 34(4):66, 2015.
- [29] J. Solomon, R. Rustamov, L. Guibas, and A. Butscher. Earth mover’s distances on discrete surfaces. *ACM Transactions on Graphics (TOG)*, 33(4):67, 2014.
- [30] J. Solomon, R. Rustamov, L. Guibas, and A. Butscher. Wasserstein propagation for semi-supervised learning. In *International Conference on Machine Learning (ICML)*, 2014.
- [31] I. Sutskever, J. Martens, G. E. Dahl, and G. E. Hinton. On the importance of initialization and momentum in deep learning. In *International Conference on Machine Learning (ICML)*, 2013.
- [32] S. Vallender. Calculation of the wasserstein distance between probability distributions on the line. *Theory of Probability & Its Applications*, 18(4):784–786, 1974.
- [33] C. Villani. *Optimal transport: old and new*, volume 338. Springer Science & Business Media, 2008.